HHS Public Access

Author manuscript

Pediatr Radiol. Author manuscript; available in PMC 2024 October 07.

Published in final edited form as:

Pediatr Radiol. 2021 November ; 51(12): 2270–2283. doi:10.1007/s00247-021-04974-4.

Contrast-enhanced ultrasound of the pediatric brain

Misun Hwang[1,2], **Carol E. Barnewolt**[3], **Jörg Jüngert**[4], **Francesco Prada**[5,6,7], **Anush Sridharan**[1], **Ryne A. Didier**[1,2]

[1]Department of Radiology, Children's Hospital of Philadelphia, 3401 Civic Center Blvd., Philadelphia, PA 19104, USA

[2]Perelman School of Medicine, University of Pennsylvania, Philadelphia, PA, USA

[3]Department of Radiology, Boston Children's Hospital, Harvard University, Boston, MA, USA

[4]Department of Pediatrics, Friedrich-Alexander University Erlangen – Nürnberg, Erlangen, Germany

[5]Acoustic Neuroimaging and Therapy Laboratory, Fondazione IRCCS Istituto Neurologico Carlo Besta, Milan, Italy

[6]Department of Neurological Surgery, University of Virginia School of Medicine, Charlottesville, VA, USA

[7]Focused Ultrasound Foundation, Charlottesville, VA, USA

Abstract

Brain contrast-enhanced ultrasound (CEUS) is an emerging application that can complement gray-scale US and yield additional insights into cerebral flow dynamics. CEUS uses intravenous injection of ultrasound contrast agents (UCAs) to highlight tissue perfUsion and thus more clearly delineate cerebral pathologies including stroke, hypoxic–ischemic injury and focal lesions such as tumors and vascular malformations. It can be applied not only in infants with open fontanelles but also in older children and adults via a transtemporal window or surgically created acoustic window. Advancements in CEUS technology and post-processing methods for quantitative analysis of UCA kinetics further elucidate cerebral microcirculation. In this review article we discuss the CEUS examination protocol for brain imaging in children, current clinical applications and future directions for research and clinical uses of brain CEUS.

Keywords

Brain; Children; Contrast-enhanced ultrasound; Epilepsy; Hypoxic–ischemic injury; Neurovascular disease; Stroke; Tumor; Ultrasound; Ultrasound contrast agents

Misun Hwang, hwangm@email.chop.edu.

Conflicts of interest None

Introduction

Brain contrast-enhanced ultrasound (CEUS) is an emerging application with much potential. The intravenous (IV) administration of ultrasound contrast agents (UCAs) composed of tiny microbubbles permits qualitative and quantitative evaluation of cerebral perfusion, which is altered in a variety of intracranial pathologies [1, 2].

Although Doppler US is the first-line tool to image cerebral flow dynamics in infants, it has certain inherent limitations. Doppler US measures macrovascular flow and is less sensitive to slow-flow conditions prevalent in microvasculature. It is also more prone to motion-related artifacts. CEUS can solve this problem by assessing cerebral tissue perfusion at the microvascular level, thus increasing the conspicuity of pathologies affecting cerebral macro- and microcirculation [3].

Contrast-enhanced US allows visualization of dynamic perfusion in the whole brain at bedside, which can be a useful adjunct not only to color Doppler, but to MRI as well. When CEUS is combined with quantitative analysis, evaluation of cerebral microvasculature at superb resolution is feasible, enabling new insights into various neurologic diseases and improving diagnostic accuracy and prognostication. Already brain CEUS has shown much promise in applications to a variety of clinical indications in children and adults such as stroke, hypoxic-ischemic injury and brain tumors [2, 4, 5]. Further clinical experience as well as preclinical and clinical research is expected to facilitate the regulatory approval of brain CEUS and widen its applications.

This article reviews the current knowledge of brain CEUS, focusing on examination protocol, basic quantification methods and clinical applications. We emphasize applications of CEUS in the pediatric population in order to examine how it can be used to improve care for these children.

Examination technique

Pre-contrast scan

Prior to CEUS, a standard gray-scale brain US is typically performed to screen for intracranial pathology or evaluate the region of concern (e.g., tumor, vascular malformation). This initial identification and localization of focal intracranial abnormality can help tailor the subsequent brain CEUS protocol such that dedicated static and cine clips of the area of interest are acquired. In the setting when focal abnormality is not evident on gray-scale US images, the brain CEUS protocol is modified to incorporate cine clips through the whole brain to screen for potential abnormality.

Ultrasound contrast agent dosing

Lumason (Bracco Diagnostics Inc., Monroe Township, NJ) is the only commercially available UCA approved for pediatric use by the United States Food and Drug Administration (FDA) in the evaluation of focal liver lesions and echocardiography following intravenous (IV) administration. In the clinical and research settings for pediatric brain imaging, however, Lumason and all other commercially available UCAs, including

Definity (Lantheus Medical Imaging, North Billerica, MA) and Optison (GE Healthcare, Princeton, NJ), have been used off-label [4, 6-10]. For brain CEUS applications, a wide range of dosing schemes has been used, including bolus injections ranging up to 6.25 mL and infusion-based administrations at rates up to 0.80 mL/s [2]. While fewer studies are available on the application of brain CEUS in infants, the same dosing recommended for IV liver imaging and echocardiography, a bolus injection of Lumason at 0.03 mL/kg, has been safely used for diagnostic evaluation of brain injury [4]. As with abdominal indications, dosage might need to be adjusted depending on the exam goals and the child's weight [11]. If the exam goal is to characterize microvascular flow dynamics using advanced particle tracking methods, in which individual intravascular microbubbles are tracked across multiple US frames to generate a vascular map of microcirculatory flow, injection dosage is smaller than that used for diagnostic evaluation [12, 13]. In addition, as compared to an older child or adult, an infant would require a smaller dose for characterizing brain perfusion abnormality because of the infant's smaller brain volume and thus smaller intravascular volume for opacification [4, 8]. Bolus injection can be performed up to twice, with the second injection dedicated to confirming the findings of the first injection, validating reproducibility or performing additional screening of perfusion abnormalities in regions not explored or carefully evaluated during the first injection.

Ultrasound contrast agent administration

Most brain CEUS studies on children and adults to date have used a bolus-based UCA injection technique, with a smaller number of studies having utilized the infusion-based technique [2]. Currently, there are no standardized guidelines on the bolus- or infusion-based techniques for the off-label application of CEUS to the brain. If the infusion administration method is used, UCA can be injected using an infusion pump or gravity-based drip infusion from a bag of UCA/saline solution. The infusion method can be helpful for intraoperative brain CEUS and for application of advanced particle tracking analysis for super-resolution microvascular imaging [12-15]. Unlike the infusion technique, the bolus technique allows characterization of UCA washout, which is an important metric in cerebral pathologies including hypoxic–ischemic injury [16]. With the bolus technique, it is important to stress the need for adequate saline flush to advance the microbubbles beyond the IV tubing. In the case of infants or smaller children, the smaller-gauge IV lines necessitate slower injection of UCA so as not to destroy microbubbles from shear stress. With both bolus and infusion methods, technical variability can arise from differing rates of injection, length of IV line, microbubbles' concentration, injection set-up, and the type of syringes used for UCA administration [17-22]. Consequently, qualitative and quantitative interpretation can be affected. Standardization of UCA administration can minimize such variability. However, in the intensive care unit environment, it is often difficult to control all these factors. Documentation of potential sources of technical variability in such a setting might be helpful for data interpretation.

Brain contrast-enhanced ultrasound examination

Transducers

In infants with open fontanelles and children and adults with closed fontanelles, brain CEUS is performed with a sector or curved-array transducer with an approximate frequency range of 2–8 MHz. Evaluation of extra-axial space, dural venous sinus and superficial brain structures can be carried out using a linear-array transducer with an approximate frequency range of 8–15 MHz.

Settings

Image settings are optimized before contrast injection. Low mechanical index (<0.3) during CEUS ensures microbubble stability. The focal zone is set deep to the region of interest so as not to prematurely destroy microbubbles in the imaged field of view. The depth is set on the reference gray-scale US image for coverage of the entire brain in the field of view. Gain is adjusted to ensure that background noise is minimal prior to contrast administration.

Fontanelles

In infants, open fontanelles serve as an acoustic window for brain exams. The anterior fontanelle is most commonly used, from which static images and cine clips of the brain in coronal and sagittal planes can be obtained. The posterior and mastoid fontanelles provide additional acoustic windows through which further views can be acquired. Older children do not have open fontanelles so an acoustic window is best achieved through the temporal bone, the thinnest bone in the skull [11]. The qualitative and quantitative interpretation of UCA intensity through the transtemporal approach is feasible, though the presence of bone decreases UCA signal and resolution because of its high acoustic impedance mismatch and associated US artifacts [2, 23]. In the future, technical optimization — either by modifying the transducer design or placing external metamaterial over the skull — to reduce the acoustic interference by bone might be helpful [24]. In addition to the transtemporal window, a craniotomy can be used intraoperatively for brain CEUS imaging in children and adults with closed fontanelles. In this case a sterile cover can be applied to allow imaging through the craniotomy site [5, 14, 25, 26].

Brain contrast-enhanced ultrasound protocol for infants with open Fontanelle —To screen for potential perfusion abnormality in the brain, the initial cine clip — in the mid-coronal plane with the basal ganglia in view — is obtained until maximum contrast enhancement is reached [1]. This is followed by an anterior-to-posterior sweep of the brain to screen for perfusion abnormalities in the remainder of the brain parenchyma. A second microbubble injection can be used to perform another sweep through the brain during peak enhancement to validate the findings from the first injection or re-evaluate the brain. For evaluation of a known region of abnormality, dedicated static and cine images of the region of interest can be obtained.

Brain contrast-enhanced ultrasound protocol for children and adults with closed Fontanelle—For screening of intracranial abnormality in children and adults with closed fontanelles, an initial cine clip of approximately 15–20 s in length should be

obtained, first via the transtemporal approach in the mid axial plane to confirm appropriate wash-in of contrast agent. After confirmation of peak enhancement and early washout of contrast agent, cine clips of the whole brain are obtained to screen for potential perfusion abnormality. The probe can be tilted superiorly and inferiorly through the transtemporal window to acquire axial scans through the whole brain. The acquisition of sweeps through the brain immediately following confirmation of early washout ensures that injury-related delay in washout is not occurring and that perfusion abnormalities are accentuated [1, 2]. The scanning approach can be modified depending on the clinical indication. For instance, a brain CEUS exam meant to monitor a known tumor would be tailored to use static images and cine clips to target the tumor and its surrounding parenchyma [14]. To screen for additional lesions in the brain, sweeps through the brain can be obtained during peak enhancement and washout phases.

Brain contrast-enhanced ultrasound protocol for intraoperative imaging

In intraoperative brain CEUS, after bone flap removal, a US probe of suitable size and frequency is placed directly on the intact meninges for transdural imaging. A small linear-array multi-frequency transducer with linear or trapezoidal views can be used for additional views. For smaller surgical accesses or when exploring the surgical cavity, a small micro-convex multi-frequency transducer might be necessary. Intraoperative CEUS imaging settings are adapted for each case accordingly. In the future, MRI–CEUS fusion imaging might be explored as a means to better localize and characterize the perfusion characteristics of focal intracranial lesions in the intraoperative setting [27]. Brain CEUS complements MRI by helping to localize lesions intraoperatively with its ability to depict tissue perfusion, particularly when only limited MRI anatomical sequences are available.

Quantification methods

The conventional time-intensity curve analysis, which assesses changes in microbubble intensity over time in a region of interest, permits quantification of tissue perfusion [28]. The basic perfusion kinetics parameters include time to peak (time it takes for microbubbles to reach peak enhancement), wash-in slope (the rate at which microbubbles wash in), peak intensity or enhancement (the highest microbubble intensity achieved), wash-in area under the curve (the total volume of microbubbles from injection to peak enhancement), washout area under the curve (the total volume of microbubbles from peak enhancement to wash out), and washout slope (the rate at which microbubbles wash out) (Fig. 1). These time-intensity-curve-based perfusion parameters are represented as a color-coded map such that spatiotemporal variations in perfusion kinetics parameters are visually apparent [29-31].

In a normal brain, peak enhancement is typically obtained within 15–20 s of UCA injection (time to peak), though there is some variability in this timing as a result of the injection site, rate of injection, length of intravenous line and systemic hemodynamics [1]. Further work is needed to establish age-appropriate, region-specific normative values for peak enhancement and area under the curve. Complete washout occurs within approximately 10 min of microbubble injection in normal infants. Depending on the type and severity of brain injury, washout can be delayed to variable degrees. In the severely injured brain, for

instance, washout can be delayed by seconds or even minutes. In the presence of raised intracranial pressure near brain death, washout might not be observed even after 30 min of scanning [16]. The washout phase can be divided into early and late periods. Although there is standardized timing for early and late washout in the evaluation of focal liver lesions (with early washout referring to <60 s and late washout to >60 s after UCA injection), further work is needed to define clinically meaningful early and late washout periods for various brain CEUS indications.

In an infusion-based destruction-replenishment method, tissue perfusion is measured at steady state; in this scheme, microbubbles in the field of imaging are destroyed and replenishment kinetics are studied (Fig. 1). By applying a short acoustic pulse higher in power (approximate mechanical index of 1.0–1.5) than that used for CEUS imaging, microbubbles in the field of view are destroyed, and this is followed by replenishment of circulating microbubbles into the same region.

Safety

To date, no serious adverse event has been reported in brain CEUS literature encompassing more than 800 children and adults [2]. Like gray-scale and color Doppler US, brain CEUS has been performed in critically ill infants and in the intraoperative setting because MRI in these settings is practically challenging. Brain CEUS, as compared to brain CT or MRI with contrast agent, is a safe option for the pediatric population and obviates the risks associated with transport or sedation [1, 2]. Sedation, particularly, can be harmful to the vulnerable, rapidly maturing brain of infants. There is a theoretical risk associated with microbubble cavitation, which refers to microbubble destruction caused by high acoustic power (mechanical index >0.8) resulting in potential thermal or mechanical bioeffects [32]. However, studies on large animal models validating the potential bioeffects of diagnostic CEUS settings in brain are not available and further exploration is warranted. The destruction scheme uses a similar mechanical index as in gray-scale US and lasts several seconds at most. Previously reported computational models, in vitro settings, and small animal models using prolonged imaging times or higher mechanical index are not accurate representations of the potential bioeffects from diagnostic brain CEUS applied to humans [32]. However, even when rapid, short pulses that are higher than clinically used mechanical index have been used for therapeutic applications, such as the opening of the blood-brain barrier, no significant histological bioeffects have been observed [33].

Clinical applications

Hypoxic–ischemic injury

Hypoxic–ischemic injury contributes significantly to morbidity and mortality in the neonatal population, with an incidence of 3 per 1,000 live births in developed countries [34]. Hypoxic–ischemic injury is one of the common causes of long-term neurologic dysfunction in children after cardiac arrest [35, 36]. Therefore, early diagnosis and treatment of hypoxic–ischemic injury is crucial for improved clinical management and prognostication of short- and long-term outcomes. Currently, MRI is recognized as the most sensitive and specific imaging technique for evaluation of neurologic pathology in hypoxic–ischemic injury [37,

38]. The acute changes of a hypoxic–ischemic event are best appreciated on diffusion-weighted imaging (DWI) [39, 40]. In the early subacute stage, both T1 and T2 sequences demonstrate hyperintensity in injured areas [39]. Beyond these conventional MRI sequences, MR spectroscopy, diffusion tensor imaging (DTI) and arterial spin-labeled perfusion-weighted imaging have been used to diagnose and prognosticate hypoxic–ischemic injury [41-47].

While further work is needed to validate the diagnostic utility and prognostic value of brain CEUS in the evaluation of hypoxic–ischemic injury, preliminary evidence in infants and children suggests that it has the potential to serve as a nimble bedside tool, complementary to MRI [4]. With CEUS, hypoxic–ischemic injury is diagnosed based on detecting secondary perfusion changes associated with the injury. With hypoxic–ischemic insult, there is an initial decrease in perfusion in the hyperacute phase followed by reperfusion in the acute/subacute phases, which is sometimes restorative to the injured tissues depending on the extent to which reperfusion injury occurs. The chronic phase of injury might demonstrate restoration or decreased perfusion, the latter from the permanent brain damage resulting from severe hypoxic–ischemic insult [48]. In addition, emerging evidence suggests that poor outcome can be predicted by exaggerated hypo- or hyperperfusion response to hypoxic–ischemic injury in the absence of changes on conventional MRI sequences (either diffusion-weighted or T1–/T2-weighted) [49, 50]. Indeed, alterations in cerebral perfusion and subsequent brain injury can be caused by impaired cerebral autoregulation, reperfusion or secondary injury, microangiopathy, raised intracranial pressure or metabolic dysfunction, all of which might not be readily evident on conventional MRI [13, 51-54].

Prior to the implementation of brain CEUS, three challenges are worth recognizing. First, perfusion response to hypoxic–ischemic injury can be variable depending on the timing of injury, evolving pathophysiology, and ongoing therapy such as hypothermia. Second, perfusion abnormalities associated with hypoxic–ischemic injury can be symmetrical or diffuse, in which case both qualitative and quantitative evaluations can be challenging because of the lack of a reliable internal control. However, this can be overcome by developing age-specific normative brain CEUS perfusion values. Third, perfusion changes on MRI in the absence of conventional MRI findings can occur because of the complexity of cerebrovascular physiology and subtle nature of some injuries that are only evident on advanced MRI techniques such as MR spectroscopy or DTI [41, 49, 50, 55, 56]. This means that using conventional MRI, specifically diffusion or T1/T2-weighted sequences, as the reference standard test for the presence or absence of hypoxic–ischemic injury is not always appropriate. The application of brain CEUS for hypoxic–ischemic injury should be performed with the understanding that perfusion is a dynamic phenomenon that can be altered by multiple factors, including the timing and extent of injury. Ideally, the potential clinical utility of brain CEUS should be assessed in the context of advanced MRI techniques and clinical outcomes, rather than relying on conventional MRI alone as the reference standard.

In the evaluation of hypoxic–ischemic injury, Hwang et al. [4] introduced a quantitative CEUS approach to screening for the presence of hypoxic–ischemic injury. Unaffected infants were distinguished from those with hypoxic–ischemic injury by assessing the

ratio of central gray nuclei to cortical perfusion using wash-in, peak enhancement and area-under-the-curve kinetics parameters on the time-intensity curve. This quantitative approach is based on the knowledge that infants have relatively more avid perfusion to the central gray nuclei than the cortex, with a central-gray-nuclei–to–cortex perfusion ratio >1. Alteration of this perfusion pattern can be seen in hypoxic–ischemic injury (Fig. 2). In rare instances, the injury can affect the cortex and central gray nuclei to similar extents, resulting in commensurate perfusion changes that do not alter the central-gray-nuclei–to–cortex perfusion ratio. Future research into creating quantitative methods for detecting injuries at the regional level, even in mixed injury patterns, might be helpful. Furthermore, availability of reference standard values of brain perfusion would support detection of these challenging cases.

Congenital heart disease

Congenital heart disease affects approximately 40,000 births per year in the United States [57, 58]. It is the leading cause of infant mortality from birth defects [59]. In a report of infant mortality during the period spanning 2003–2006, 4.2% of all neonatal deaths were caused by a congenital heart defect [60]. In this report, hypoplastic left heart syndrome accounted for the majority of mortality, followed by other conditions such as the transposition of the great vessels and ventricular septal defect. In 2009 pediatric hospitalizations caused by congenital heart disease cost $5.6 billion and accounted for 15% of costs for all pediatric hospitalizations [59]. While advancements in medical and surgical care of children with congenital heart disease have resulted in improved survival, long-term neurocognitive impairment is a growing concern in this population [61].

The effects of complex congenital heart disease and surgical intervention on the growing brain remain poorly understood. Along with the results of neonatal heart surgery, the effects of surgery on the brain should therefore be carefully monitored in the intraoperative and postoperative periods because the risk of long-term neurologic developmental impairment is high [15, 62]. There is increased prevalence of brain injury after surgical intervention [63-66]. In the wide spectrum of neuroimaging abnormalities, periventricular leukomalacia is most common; it is postulated that this is because of the enhanced vulnerability of premyelinating oligodendrocyte precursor cells to hypoxic insult [63, 65, 66]. Prognostic tools for infants with congenital heart disease are highly desired and the subject of numerous studies [67-72]. Baseline brain perfusion prior to surgery differs among infants with various types of congenital heart disease. Accurate understanding of these perfusion patterns should improve prognostication of long-term neurodevelopmental outcomes. Such understanding could impact the timing of surgical management in infants requiring staged interventions.

In terms of the current neuroimaging algorithm, brain MRI is often performed because of the high prevalence of central nervous system abnormalities in this population. Multimodal approaches to intraoperative neuromonitoring have been reported, using techniques such as near-infrared spectroscopy, transcranial Doppler US, and electroencephalogram (EEG) [73, 74]. As compared to these modalities, brain CEUS helps delineate brain perfusion at the global and regional levels; thus, brain CEUS can serve as a useful technique for intraoperative monitoring of brain perfusion during neonatal cardiac surgery (Figs. 3 and

4) [15]. For the future, baseline, intraoperative and post-surgical brain perfusion might be compared in correlation to long-term clinical outcomes.

Stroke

Pediatric stroke, while rare, is associated with significant mortality and morbidity. The incidence of combined ischemic and hemorrhagic pediatric stroke is reportedly up to 13 cases per 100,000 children [75-78]. Approximately 10–25% of children affected by stroke will die, while up to 66% of them will live with persistent neurologic deficits and neurodevelopmental problems [79, 80]. As a result, caring for these children involves a substantial financial and emotional burden for families and society [81]. To improve clinical outcomes in pediatric stroke, reliable neurodiagnostic tools for early recognition and therapeutic guidance are much needed.

Magnetic resonance perfusion imaging has traditionally been used for assessing acute stroke in pediatric and adult patients. However, risks associated with transportation, incompatible support equipment, and potential need for sedation or anesthesia can limit MRI utilization in critically ill children. Non-contrast CT and contrast-enhanced CT angiography have also been performed but are not preferred in children because of the potential risks of radiation and transportation. CEUS has superior spatial resolution for evaluating microvasculature brain perfusion. Thus the combination of noninvasive bedside evaluation with US and CEUS offers advantages over CT and MRI in these children. CEUS evaluation of acute ischemic stroke has been reported predominantly in adults and can be used to detect cerebral perfusion deficits in acute ischemic stroke or to monitor response to thrombolysis treatment [23, 82]. Although few studies have evaluated pediatric stroke with brain CEUS, such an application is conceivable and is an area of future research.

If there is a concern for stroke, the mid axial plane for imaging through the central basal ganglia can be performed initially. Note that depending on the timing of stroke and the tissue characteristics (tissue at risk versus injured tissue), cerebral perfusion as assessed with quantitative brain CEUS can be different. As seen in hypoxic–ischemic injury, UCA transit through the brain vasculature can be slowed in stroke, resulting in delayed mean transit time on MRI or delayed rate of washout on CEUS [83]. Delayed time to peak is another quantitative finding reported in the tissue affected by acute stroke using brain CEUS [23]. Comparison of the quantitative perfusion parameters between the affected and non-affected sides can be informative in the diagnosis of stroke and monitoring for reperfusion during thrombolytic therapy [23]. To screen for potential involvement of other vascular territories in the remainder of the brain, the examiner can perform superior-to-inferior sweeps on the axial plane. Larger prospective studies are needed to compare the diagnostic accuracy of CEUS and MRI in the detection of stroke, and the utility of CEUS for accurate characterization of the penumbra for thrombolytic therapy. Establishing robust quantitative approaches to diagnosing and serially monitoring the ischemic core and penumbra might be valuable to guiding post-stroke therapy.

Brain tumors

Central nervous system (CNS) tumors are the leading cause of cancer death in children ages 0–14 years in the United States, with a tumor incidence of 5.5 cases per 100,000 [84]. Primary pediatric spinal cord tumors are rare, with a frequency of 0.2 per 100,000 person-years. The incidence of these neoplasms increases from ages 0–4 years (0.2 per 100,000 person-years) to ages 15–19 years (0.3 per 100,000 person-years) [85]. Surgical removal represents a therapeutic option in a large number of cases.

Brain MRI is the gold standard for initial diagnostic assessment and follow-up of brain tumors in children. The utility of brain CEUS has been shown predominantly in the intraoperative setting when brain MRI cannot be easily performed. Intraoperative CEUS during adult neurosurgical procedures was performed for the first time in 2005 by Kanno et al. [86]. In this study, a first-generation UCA was used to enhance power Doppler imaging to highlight brain tumors, applying the transducer directly over the meninges after craniotomy. Since this preliminary experience, other authors have explored the potential of intraoperative CEUS to guide neurosurgical procedures, mainly enhancing tumor visualization and delineating vascular landmarks for guiding tumor resection. The intraoperative CEUS in neurosurgical practice has been incorporated into the European Federation of Societies for Ultrasound in Medicine and Biology guidelines [87]. The first use of intraoperative CEUS in a pediatric neurosurgical patient was reported in 2015, describing the case of a 14-year-old boy who underwent operation for an intramedullary cervical spine tumor [88]. Indeed, with adequate knowledge, the advantages encountered in the adult population with the use of intraoperative CEUS technique in neurosurgical procedures can be translated to the pediatric population.

US has proved to be a useful, portable tool to guide surgical removal of CNS tumors, but its utility for discerning tumor and normal neural parenchyma is limited. To this end, intraoperative CEUS has shown potential to highlight neoplastic tissue in adults [14, 25, 26, 86, 88-94]. A direct comparison between intraoperative CEUS and T1-W gadolinium-enhanced MRI using fusion imaging demonstrated that the former shows the same tumoral location and volume as MRI, demonstrating that intraoperative CEUS can be reliably used for surgical guidance [95] (Fig. 5). Neoplastic tissue might demonstrate higher intraoperative CEUS contrast enhancement because of its higher vessel density compared to the normal surrounding brain parenchyma, although the presence of necrosis would reduce the tumoral enhancement [96].

Studies have also showed that brain CEUS allows for differentiation of tumor from edema as well as detection of residual tumor [93, 96]. As compared to cerebral edema, low-grade glioma demonstrated higher enhancement and faster time to peak [96]. Furthermore, when coupled with MRI–CEUS fusion imaging for virtual navigation, CEUS allowed for localization of major vessels within the surgical field, which aids in the visualization of feeding vessels prior to the start of tumor resection. This allows precise devascularization of the tumor and reduces blood loss, which is crucial in children for avoiding severe hemodynamic dysfunction. Because microbubbles behave as purely intravascular contrast media that do not spread into the interstitial space, intraoperative CEUS can be employed as

a real-time tool in the surgical field to display both large and small vessels and to allow for assessment of tissue perfusion during cranial tumor surgery [14, 92].

Epilepsy

Epilepsy is the most common chronic neurologic condition in children [97]. The incidence of epilepsy in children ranges 3.2–5.5 per 1,000 in developed countries [98]. Epilepsy is characterized by unpredictable and often short-lasting repetitive epileptic seizures that can be life-threatening. There is a wide spectrum of neuropathological alterations and clinical phenomenology [99]. Children with epilepsy, even those with milder forms of the disease, suffer from lifestyle limitations and social stigmatization [100].

Video-electroencephalography (VEEG) monitoring is the gold standard for diagnostic evaluation of seizures [101]. Video adds benefit to EEG because the video might demonstrate behavioral phenomena associated with seizures. Both VEEG and EEG can continuously record electrical activity; however, precise spatial localization of the ictal focus with these methods can be difficult and data can be degraded by artifacts [102]. Pilot studies have used cerebral blood flow measurements of ictal activation using thermal diffusion flowmetry and near-infrared spectroscopy, but these need further validation to be translated into the clinical setting [103, 104]. Note also that MRI is not able to identify an etiological lesion in up to 40% or more cases [105]. Single-photon emission CT and positron emission tomography have been used for ictal and interictal imaging, but as with MRI, these are not portable tools and are not readily accessible during seizures [106].

There is a paucity of data on the application of brain CEUS for diagnostic evaluation of epilepsy. Yet, theoretically, brain CEUS would assist with intraoperative localization of focal lesions responsible for epilepsy. It would be interesting to study whether brain CEUS can serve as a tool for localization of an ictal focus, with or without an associated anatomically evident lesion on MRI. In terms of an anatomically evident ictal focus, focal cortical dysplasia is the most common cause of symptomatic drug-resistant epilepsy, and surgery can achieve seizure control. However, intraoperative identification of the tissue to be resected can be challenging [107]. Usually these developmental anomalies harbor a higher number of functional microvessels compared to the surrounding cerebral cortex, facilitating identification of these regions on CEUS. Thus intraoperative CEUS could be employed as an adjunct tool to advanced imaging to visualize the dysplastic area, guiding total resection. The same concept applies to other lesions, such as the dysembryoplastic neuroepithelial tumor, that can induce drug-resistant epilepsy. When a clear lesion is not observed, disconnection or resection procedures are necessary. In such cases, vessels can serve as landmarks, and their identification as well as their sparing is mandatory; here, too, the use of intraoperative CEUS to visualize all vessels in the surgical field could guide and help the resection.

Neurovascular diseases

Pediatric neurovascular diseases encompass a wide spectrum of pathologies affecting small and large vessels of the brain in children [108-110]. While neurovascular disease is less common in children than in adults, pathological evidence suggests that it is a more common

entity than has been reported [111]. The disease can be diffuse or focal. Potential etiologies for diffuse involvement of small or large vessels include congenital heart defects, post hypoxia or traumatic microthrombi from hypercoagulability, rheumatologic mechanisms, connective tissue disorders, genetic mutations, infectious or inflammatory vasculitis, and those related to treatment (e.g., radiation and chemotherapy) [54, 108-110]. Focal or multifocal lesions can be genetic, developmental, sporadic or acquired. Some examples include cavernous malformation, arteriovenous malformation, hereditary hemorrhagic telangiectasia and vein of Galen malformation [109].

The gold standard exam used for screening and workup of pediatric neurovascular diseases is brain MRI. In situations when there is a known focal vascular lesion in the brain, brain CEUS can be complementary to MRI and can be used for intraoperative guidance and monitoring of the lesion. Intraoperative CEUS is superior to Doppler US in helping to localize small branches and can provide information about aneurysmal sac morphology and orientation, arteriovenous malformation nidus, and flow in proximal and distal vessels. Intraoperative brain CEUS can also be helpful during revascularization surgery in cases such as moyamoya disease, a cerebrovascular syndrome characterized by progressive stenosis of the intracranial internal carotid arteries and their proximal branches, that predispose to ischemic and hemorrhagic events [112]. In combination with other intraoperative imaging techniques, intraoperative CEUS can be used to assess stenosis of the internal carotid artery and its distal branches, evaluate tissue perfusion and confirm the patency of the bypass [113].

After lesion excision or neurovascular lesion embolization, brain CEUS can assess residual flow within the nidus or vessels supplying and draining the nidus in arteriovenous malformation surgery (Fig. 6) [25, 26, 114]. The utilization of brain CEUS helps to avoid more invasive or time-consuming examinations, with the added advantage of reducing radiation exposure and iodinated contrast agents in children [115]. Serial monitoring can be conveniently done at bedside or clinic visits in a cost-effective manner. For the future, the development of three-dimensional technology for CEUS imaging would prove to be helpful in the reconstruction of vascular morphology in a similar manner to CT or MRI. Analogous to MRI or CT angiography, maximum-intensity projections (MIP) of brain CEUS can be obtained during wash-in of contrast agent to reconstruct neurovascular architecture. Following UCA injection, the MIP technique selects maximum pixel intensity over consecutive CEUS images to generate a composite vascular map. The CEUS-based MIP technique has been used in a variety of human applications, including breast, prostate, liver and brain [15, 116-119]. Future explorations of brain CEUS MIP might prove useful for diagnostic evaluation of pediatric neurovascular diseases.

As for the diagnostic accuracy of brain CEUS in screening for focal or diffuse neurovascular diseases, further studies are warranted. This necessitates increased familiarization with normal neurovascular anatomy on brain CEUS, technological advancements to instantaneously generate a neurovascular map at bedside, and prospective studies comparing brain CEUS to the reference standard brain MRI for initial validation.

Conclusion

Brain CEUS can be a useful tool for evaluating various central nervous system pathologies affecting children and can serve as an adjunct modality to MRI or CT. Current evidence suggests that with the appropriate scan settings, the potential risk involved in performing brain CEUS is minimal and lower than that associated with other contrast agents such as iodinated contrast and gadolinium. Because of its utility for assessing cerebral perfusion at the macro- and microvascular levels, brain CEUS offers distinct functional insights into the cerebral tissue and associated pathologies important for disease diagnosis and prognosis. Beyond the attempts to achieve diagnostic equivalence or superiority as compared to existing advanced modalities, other interesting research would be to explore whether CEUS can detect brain injury early and improve prognostication. Further clinical experience and research on the diagnostic and prognostic value of brain CEUS is therefore much warranted.

References

1. Hwang M (2018) Introduction to contrast-enhanced ultrasound of the brain in neonates and infants: current understanding and future potential. Pediatr Radiol 49:254–262 [PubMed: 30353273]
2. Vinke EJ, Kortenbout AJ, Eyding J et al. (2017) Potential of contrast-enhanced ultrasound as a bedside monitoring technique in cerebral perfusion: a systematic review. Ultrasound Med Biol 43:2751–2757 [PubMed: 28964614]
3. Archer LN, Levene MI, Evans DH(1986) Cerebral artery Doppler ultrasonography for prediction of outcome after perinatal asphyxia. Lancet 2:1116–1118 [PubMed: 2877270]
4. Hwang M, Sridharan A, Darge K et al. (2019) Novel quantitative contrast-enhanced ultrasound detection of hypoxic ischemic injury in neonates and infants: pilot study 1. J Ultrasound Med 38: 2025–2038 [PubMed: 30560547]
5. Prada F, Bene MD, Fornaro R et al. (2016) Identification of residual tumor with intraoperative contrast-enhanced ultrasound during glioblastoma resection. Neurosurg Focus 40:E7
6. Kern R, Diels A, Pettenpohl J et al. (2011) Real-time ultrasound brain perfusion imaging with analysis of microbubble replenishment in acute MCA stroke. J Cereb Blood Flow Metab 31:1716–1724 [PubMed: 21364598]
7. Meves SH, Wilkening W, Thies T et al. (2002) Comparison between echo contrast agent-specific imaging modes and perfusion-weighted magnetic resonance imaging for the assessment of brain perfusion. Stroke 33:2433–2437 [PubMed: 12364734]
8. Puls I, Hauck K, Demuth K et al. (1999) Diagnostic impact of cerebral transit time in the identification of microangiopathy in dementia: a transcranial ultrasound study. Stroke 30:2291–2295 [PubMed: 10548660]
9. Jungehulsing GJ, Brunecker P, Nolte CH et al. (2008) Diagnostic transcranial ultrasound perfusion-imaging at 2.5 MHz does not affect the blood–brain barrier. Ultrasound Med Biol 34:147–150 [PubMed: 17854981]
10. Holscher T, Wilkening W, Draganski B et al. (2005) Transcranial ultrasound brain perfusion assessment with a contrast agent-specific imaging mode: results of a two-center trial. Stroke 36:2283–2285 [PubMed: 16141430]
11. Hwang M, Riggs BJ, Katz J et al. (2018) Advanced pediatric neurosonography techniques: contrast-enhanced ultrasonography, elastography, and beyond. J Neuroimaging 28:150–157 [PubMed: 29280236]
12. Christensen-Jeffries K, Couture O, Dayton PA et al. (2020) Super-resolution ultrasound imaging. Ultrasound Med Biol 46:865–891 [PubMed: 31973952]
13. Zhang Z, Katz J, Hwang M et al. (2019) Cerebral vasculars super resolution imaging and blood flow measurement using ultrasound enhanced particle tracking velocimetry. 72nd annual meeting of the APS division of fluid dynamics, Seattle

14. Prada F, Perin A, Martegani A et al. (2014) Intraoperative contrast-enhanced ultrasound for brain tumor surgery. Neurosurgery 74:542–552 [PubMed: 24598809]
15. Knieling F, Ruffer A, Cesnjevar R et al. (2020) Transfontanellar contrast-enhanced ultrasound for monitoring brain perfusion during neonatal heart surgery. Circ Cardiovasc Imaging 13:e010073 [PubMed: 32114827]
16. Hwang M, Riggs BJ, Saade-Lemus S et al. (2018) Bedside contrast-enhanced ultrasound diagnosing cessation of cerebral circulation in a neonate: a novel bedside diagnostic tool. Neuroradiol J 31:578–580 [PubMed: 30189812]
17. Kramer MR, Bhagat N, Back SJ et al. (2018) Influence of contrast-enhanced ultrasound administration setups on microbubble enhancement: a focus on pediatric applications. Pediatr Radiol 48:101–108 [PubMed: 28894889]
18. Eisenbrey JR, Daecher A, Kramer MR et al. (2015) Effects of needle and catheter size on commercially available ultrasound contrast agents. J Ultrasound Med 34:1961–1968 [PubMed: 26384606]
19. Tang MX, Mulvana H, Gauthier T et al. (2011) Quantitative contrast-enhanced ultrasound imaging: a review of sources of variability. Interface Focus 1:520–539 [PubMed: 22866229]
20. Vinke EJ, Eyding J, de Korte CL et al. (2017) Repeatability of bolus kinetics ultrasound perfusion imaging for the quantification of cerebral blood flow. Ultrasound Med Biol 43:2758–2764 [PubMed: 28967502]
21. Pitre-Champagnat S, Coiffier B, Jourdain L et al. (2017) Toward a standardization of ultrasound scanners for dynamic contrast-enhanced ultrasonography: methodology and phantoms. Ultrasound Med Biol 43:2670–2677 [PubMed: 28779957]
22. Gauthier TP, Chebil M, Peronneau P et al. (2012) In vitro evaluation of the impact of ultrasound scanner settings and contrast bolus volume on time-intensity curves. Ultrasonics 52:12–19 [PubMed: 21722933]
23. Meairs S (2008) Contrast-enhanced ultrasound perfusion imaging in acute stroke patients. Eur Neurol 59:17–26 [PubMed: 18382109]
24. Shen C, Xu J, Fang NX et al. (2014) Anisotropic complementary acoustic metamaterial for canceling out aberrating layers. Phys Rev X 4:041033
25. Prada F, Del Bene M, Casali C et al. (2015) Intraoperative navigated angiosonography for skull base tumor surgery. World Neurosurg 84:1699–1707 [PubMed: 26193670]
26. Prada F, Del Bene M, Saini M et al. (2015) Intraoperative cerebral angiosonography with ultrasound contrast agents: how I do it. Acta Neurochir 157:1025–1029 [PubMed: 25854600]
27. Kearns KN, Sokolowski JD, Chadwell K et al. (2019) The role of contrast-enhanced ultrasound in neurosurgical disease. Neurosurg Focus 47:E8
28. Krix M (2008) Time intensity curves. In: Baert AL (ed) Encyclopedia of diagnostic imaging. Springer, Berlin
29. Peronneau P, Lassau N, Leguerney I et al. (2010) Contrast ultrasonography: necessity of linear data processing for the quantification of tumor vascularization. Ultraschall Med 31:370–378 [PubMed: 20577941]
30. Gauthier M, Leguerney I, Thalmensi J et al. (2011) Estimation of intra-operator variability in perfusion parameter measurements using DCE-US. World J Radiol 3:70–81 [PubMed: 21512654]
31. Pitre-Champagnat S, Leguerney I, Bosq J et al. (2015) Dynamic contrast-enhanced ultrasound parametric maps to evaluate intratumoral vascularization. Investig Radiol 50:212–217 [PubMed: 25275834]
32. Miller DL, Averkiou MA, Brayman AA et al. (2008) Bioeffects considerations for diagnostic ultrasound contrast agents. J Ultrasound Med 27:611–632 [PubMed: 18359911]
33. Morse SV, Pouliopoulos AN, Chan TG et al. (2019) Rapid short-pulse ultrasound delivers drugs uniformly across the murine blood–brain barrier with negligible disruption. Radiology 291:459–466 [PubMed: 30912718]
34. Kurinczuk JJ, White-Koning M, Badawi N (2010) Epidemiology of neonatal encephalopathy and hypoxic–ischaemic encephalopathy. Early Hum Dev 86:329–338 [PubMed: 20554402]
35. Hickey RW, Painter MJ (2006) Brain injury from cardiac arrest in children. Neurol Clin 24:147–158 [PubMed: 16443136]

36. Kirschen MP, Topjian AA, Berg RA (2016) Neurologic outcome after cardiac arrest: what you see at hospital discharge may or may not be what you get. Resuscitation 102:A1–A2 [PubMed: 26956839]
37. Sorokan ST, Jefferies AL, Miller SP (2018) Imaging the term neonatal brain. Paediatr Child Health 23:322–328 [PubMed: 30657135]
38. Intrapiromkul J, Northington F, Huisman TA et al. (2013) Accuracy of head ultrasound for the detection of intracranial hemorrhage in preterm neonates: comparison with brain MRI and susceptibility weighted imaging. J Neuroradiol 40:81–88 [PubMed: 22633043]
39. Huang BY, Castillo M (2008) Hypoxic–ischemic brain injury: imaging findings from birth to adulthood. Radiographics 28:417–439 [PubMed: 18349449]
40. Hagmann P, Jonasson L, Maeder P et al. (2006) Understanding diffusion MR imaging techniques: from scalar diffusion-weighted imaging to diffusion tensor imaging and beyond. Radiographics 26:205–223
41. Lally PJ, Montaldo P, Oliveira V et al. (2019) Magnetic resonance spectroscopy assessment of brain injury after moderate hypothermia in neonatal encephalopathy: a prospective multicentre cohort study. Lancet Neurol 18:35–45 [PubMed: 30447969]
42. De Vis JB, Hendrikse J, Petersen ET et al. (2015) Arterial spin-labelling perfusion MRI and outcome in neonates with hypoxic–ischemic encephalopathy. Eur Radiol 25:113–121 [PubMed: 25097129]
43. Massaro AN, Evangelou I, Fatemi A et al. (2015) White matter tract integrity and developmental outcome in newborn infants with hypoxic–ischemic encephalopathy treated with hypothermia. Dev Med Child Neurol 57:441–448 [PubMed: 25492527]
44. Haller S, Zaharchuk G, Thomas DL et al. (2016) Arterial spin labeling perfusion of the brain: emerging clinical applications. Radiology 281:337–356 [PubMed: 27755938]
45. Ouyang MH, Liu PY, Jeon T et al. (2017) Heterogeneous increases of regional cerebral blood flow during preterm brain development: preliminary assessment with pseudo-continuous arterial spin labeled perfusion MRI Neuroimage 147:233–242 [PubMed: 27988320]
46. Wong EC (2014) An introduction to ASL labeling techniques. J Magn Reson Imaging 40:1–10 [PubMed: 24424918]
47. Proisy M, Mitra S, Uria-Avellana C et al. (2016) Brain perfusion imaging in neonates: an overview. AJNR Am J Neuroradiol 37:1766–1773 [PubMed: 27079367]
48. Busl KM, Greer DM (2010) Hypoxic–ischemic brain injury: pathophysiology, neuropathology and mechanisms. NeuroRehabilitation 26:5–13 [PubMed: 20130351]
49. Zheng Q, Ouyang M, Martin-Saavedra JS et al. (2019) Increased brain perfusion in neonatal hypoxic ischemic injury with negative reading of DWI, T1/T2-weighted images: implications of perfusion MRI for reperfusion response monitoring and prognostication. ISMRM, Montreal
50. Wintermark P, Hansen A, Gregas MC et al. (2011) Brain perfusion in asphyxiated newborns treated with therapeutic hypothermia. AJNR Am J Neuroradiol 32:2023–2029 [PubMed: 21979494]
51. Khaw K, Sridharan A, Poznick L et al. (2020) Evaluating the correlation between bolus perfusion kinetics using contrast-enhanced ultrasound and intracranial pressure in a pediatric porcine model of asphyxia-associated cardiac arrest. Society for Pediatric Radiology Annual Meeting & Postgraduate Course, Miami
52. Mavroudis CD, Karlsson M, Ko T et al. (2018) Cerebral mitochondrial dysfunction associated with deep hypothermic circulatory arrest in neonatal swine. Eur J Cardiothorac Surg 54:162–168 [PubMed: 29346537]
53. Lee JK, Brady KM, Chung SE et al. (2014) A pilot study of cerebrovascular reactivity autoregulation after pediatric cardiac arrest. Resuscitation 85:1387–1393 [PubMed: 25046743]
54. Sekhon MS, Ainslie PN, Griesdale DE (2017) Clinical pathophysiology of hypoxic ischemic brain injury after cardiac arrest: a “two-hit” model. Crit Care 21:90 [PubMed: 28403909]
55. Kushwah S, Kumar A, Verma A et al. (2017) Comparison of fractional anisotropy and apparent diffusion coefficient among hypoxic ischemic encephalopathy stages 1, 2, and 3 and with nonasphyxiated newborns in 18 areas of brain. Indian J Radiol Imaging 27:447–456 [PubMed: 29379241]

56. Lemmon ME, Wagner MW, Bosemani T et al. (2017) Diffusion tensor imaging detects occult cerebellar injury in severe neonatal hypoxic-ischemic encephalopathy. Dev Neurosci 39:207–214 [PubMed: 28095379]
57. Hoffman JI, Kaplan S (2002) The incidence of congenital heart disease. J Am Coll Cardiol 39:1890–1900 [PubMed: 12084585]
58. Reller MD, Strickland MJ, Riehle-Colarusso T et al. (2008) Prevalence of congenital heart defects in metropolitan Atlanta, 1998-2005. J Pediatr 153:807–813 [PubMed: 18657826]
59. Centers for Disease Control and Prevention (2019) Data and statistics on congenital heart defects. CDC website. https://www.cdc.gov/ncbddd/heartdefects/data.html. Accessed 9 Dec 2020
60. Centers for Disease Control and Prevention (2010) Morbidity and mortality weekly report: racial differences by gestational age in neonatal deaths attributable to congenital heart defects — United States, 2003–2006. CDC website. https://www.cdc.gov/mmwr/preview/mmwrhtml/mm5937a3.htm?s_cid=mm5937a3_w. Accessed 9 Dec 2020
61. Licht DJ, Shera DM, Clancy RR et al. (2009) Brain maturation is delayed in infants with complex congenital heart defects. J Thorac Cardiovasc Surg 137:529–536 [PubMed: 19258059]
62. Best KE, Rankin J (2016) Long-term survival of individuals born with congenital heart disease: a systematic review and meta-analysis. J Am Heart Assoc 5:e002846 [PubMed: 27312802]
63. McQuillen PS, Barkovich AJ, Hamrick SE et al. (2007) Temporal and anatomic risk profile of brain injury with neonatal repair of congenital heart defects. Stroke 38:736–741 [PubMed: 17261728]
64. Newburger JW, Bellinger DC (2006) Brain injury in congenital heart disease. Circulation 113:183–185 [PubMed: 16418448]
65. Dent CL, Spaeth JP, Jones BV et al. (2005) Brain magnetic resonance imaging abnormalities after the Norwood procedure using regional cerebral perfusion. J Thorac Cardiovasc Surg 130:1523–1530 [PubMed: 16307993]
66. Mahle WT, Tavani F, Zimmerman RA et al. (2002) An MRI study of neurological injury before and after congenital heart surgery. Circulation 106:I109–I114 [PubMed: 12354718]
67. Lorusso R, Taccone FS, Belliato M et al. (2017) Brain monitoring in adult and pediatric ECMO patients: the importance of early and late assessments. Minerva Anestesiol 83:1061–1074 [PubMed: 28643997]
68. Licht DJ, Wang J, Silvestre DW et al. (2004) Preoperative cerebral blood flow is diminished in neonates with severe congenital heart defects. J Thorac Cardiovasc Surg 128:841–849 [PubMed: 15573068]
69. Zaleski KL, Kussman BD (2020) Near-infrared spectroscopy in pediatric congenital heart disease. J Cardiothorac Vasc Anesth 34: 489–500 [PubMed: 31582201]
70. Simons J, Sood ED, Derby CD et al. (2012) Predictive value of near-infrared spectroscopy on neurodevelopmental outcome after surgery for congenital heart disease in infancy. J Thorac Cardiovasc Surg 143:118–125 [PubMed: 22036260]
71. Khan MS, Fraser CD (2012) Neonatal brain protection in cardiac surgery and the role of intraoperative neuromonitoring. World J Pediatr Congenit Heart Surg 3:114–119 [PubMed: 23804694]
72. Hovels-Gurich HH (2016) Factors influencing neurodevelopment after cardiac surgery during infancy. Front Pediatr 4:137 [PubMed: 28018896]
73. Spaeder MC, Klugman D, Skurow-Todd K et al. (2017) Perioperative near-infrared spectroscopy monitoring in neonates with congenital heart disease: relationship of cerebral tissue oxygenation index variability with neurodevelopmental outcome. Pediatr Crit Care Med 18: 213–218 [PubMed: 28067688]
74. Andropoulos DB, Stayer SA, Diaz LK et al. (2004) Neurological monitoring for congenital heart surgery. Anesth Analg 99:1365–1375 [PubMed: 15502032]
75. Earley CJ, Kittner SJ, Feeser BR et al. (1998) Stroke in children and sickle-cell disease: Baltimore-Washington cooperative young stroke study. Neurology 51:169–176 [PubMed: 9674798]
76. Chung B, Wong V (2004) Pediatric stroke among Hong Kong Chinese subjects. Pediatrics 114:e206–e212 [PubMed: 15286258]

77. Schoenberg BS, Mellinger JF, Schoenberg DG (1978) Cerebrovascular disease in infants and children: a study of incidence, clinical features, and survival. Neurology 28:763–768 [PubMed: 567292]

78. Lynch JK, Hirtz DG, DeVeber G et al. (2002) Report of the National Institute of Neurological Disorders and Stroke workshop on perinatal and childhood stroke. Pediatrics 109:116–123 [PubMed: 11773550]

79. Lanthier S, Carmant L, David M et al. (2000) Stroke in children: the coexistence of multiple risk factors predicts poor outcome. Neurology 54:371–378 [PubMed: 10668698]

80. deVeber GA, MacGregor D, Curtis R et al. (2000) Neurologic outcome in survivors of childhood arterial ischemic stroke and sinovenous thrombosis. J ChildNeurol 15:316–324

81. Ellis C, McGrattan K, Mauldin P, Ovbiagele B (2014) Costs of pediatric stroke care in the United States: a systematic and contemporary review. Expert Rev Pharmacoecon Outcomes Res 14:643–650 [PubMed: 24970735]

82. Wiesmann M, Meyer K, Albers T et al. (2004) Parametric perfusion imaging with contrast-enhanced ultrasound in acute ischemic stroke. Stroke 35:508–513 [PubMed: 14739406]

83. Keedy AW, Fischette WS, Soares BP et al. (2012) Contrast delay on perfusion CT as a predictor of new, incident infarct: a retrospective cohort study. Stroke 43:1295–1301 [PubMed: 22363062]

84. Ostrom QT, de Blank PM, Kruchko C et al. (2015) Alex's Lemonade Stand Foundation infant and childhood primary brain and central nervous system tumors diagnosed in the United States in 2007–2011. Neuro Oncol 16:x1–x36 [PubMed: 25542864]

85. Sahu RK, Das KK, Bhaisora KS et al. (2015) Pediatric intramedullary spinal cord lesions: pathological spectrum and outcome of surgery. J Pediatr Neurosci 10:214–221 [PubMed: 26557160]

86. Kanno H, Ozawa Y, Sakata K et al. (2005) Intraoperative power Doppler ultrasonography with a contrast-enhancing agent for intracranial tumors. J Neurosurg 102:295–301 [PubMed: 15739558]

87. Sidhu PS, Cantisani V, Dietrich CF et al. (2018) The EFSUMB guidelines and recommendations for the clinical practice of contrast-enhanced ultrasound (CEUS) in non-hepatic applications: update 2017 (short version). Ultraschall Med 39:154–180 [PubMed: 29510440]

88. Vetrano IG, Prada F, Nataloni IF et al. (2015) Discrete or diffuse intramedullary tumor? Contrast-enhanced intraoperative ultrasound in a case of intramedullary cervicothoracic hemangioblastomas mimicking a diffuse infiltrative glioma: technical note and case report. Neurosurg Focus 39:E17

89. Holscher T, Ozgur B, Singel S et al. (2007) Intraoperative ultrasound using phase inversion harmonic imaging: first experiences. Neurosurgery 60:382–386

90. Engelhardt M, Hansen C, Eyding J et al. (2007) Feasibility of contrast-enhanced sonography during resection of cerebral tumours: initial results of a prospective study. Ultrasound Med Biol 33:571–575 [PubMed: 17337111]

91. He W, Jiang XQ, Wang S et al. (2008) Intraoperative contrast-enhanced ultrasound for brain tumors. Clin Imaging 32:419–424 [PubMed: 19006768]

92. Mattei L, Prada F, Legnani FG et al. (2016) Neurosurgical tools to extend tumor resection in hemispheric low-grade gliomas: conventional and contrast enhanced ultrasonography. Childs Nerv Syst 32:1907–1914 [PubMed: 27659832]

93. Prada F, Mattei L, Del Bene M et al. (2014) Intraoperative cerebral glioma characterization with contrast enhanced ultrasound. Biomed Res Int 2014:484261 [PubMed: 25013784]

94. Vetrano IG, Prada F, Erbetta A, DiMeco F (2015) Intraoperative ultrasound and contrast-enhanced ultrasound (CEUS) features in a case of intradural extramedullary dorsal schwannoma mimicking an intramedullary lesion. Ultraschall Med 36:307–310

95. Prada F, Vitale V, Del Bene M et al. (2017) Contrast-enhanced MR imaging versus contrast-enhanced US: a comparison in glioblastoma surgery by using intraoperative fusion imaging. Radiology 285:242–249 [PubMed: 28562204]

96. Cheng LG, He W, Zhang HX et al. (2016) Intraoperative contrast enhanced ultrasound evaluates the grade of glioma. Biomed Res Int 2016:2643862 [PubMed: 27069921]

97. Aaberg KM, Gunnes N, Bakken IJ et al. (2017) Incidence and prevalence of childhood epilepsy: a nationwide cohort study. Pediatrics 139:e20163908 [PubMed: 28557750]

98. Camfield P, Camfield C (2015) Incidence, prevalence and aetiology of seizures and epilepsy in children. Epileptic Disord 17:117–123 [PubMed: 25895502]

99. Fisher RS, van Emde BW, Blume W et al. (2005) Epileptic seizures and epilepsy: definitions proposed by the International League Against Epilepsy (ILAE) and the International Bureau for Epilepsy (IBE). Epilepsia 46:470–472 [PubMed: 15816939]

100. Beghi E (2016) Addressing the burden of epilepsy: many unmet needs. Pharmacol Res 107:79–84 [PubMed: 26952026]

101. Hamandi K, Beniczky S, Diehl B et al. (2017) Current practice and recommendations in UK epilepsy monitoring units. Report of a national survey and workshop. Seizure 50:92–98 [PubMed: 28644984]

102. Plummer C, Harvey AS, Cook M (2008) EEG source localization in focal epilepsy: where are we now? Epilepsia 49:201–218 [PubMed: 17941844]

103. Tewolde S, Oommen K, Lie DY et al. (2015) Epileptic seizure detection and prediction based on continuous cerebral blood flow monitoring — a review. J Healthc Eng 6:159–178 [PubMed: 26288885]

104. Jeppesen J, Beniczky S, Johansen P et al. (2015) Exploring the capability of wireless near infrared spectroscopy as a portable seizure detection device for epilepsy patients. Seizure 26:43–48 [PubMed: 25799901]

105. Leeman-Markowski B (2016) Review of MRI-negative epilepsy. JAMA Neurol 73:1377

106. Kim S, Mountz JM (2011) SPECT imaging of epilepsy: an overview and comparison with F-18 FDG PET. Int J Mol Imaging 2011:813028 [PubMed: 21785722]

107. Tringali G, Bono B, Dones I et al. (2018) Multimodal approach for radical excision of focal cortical dysplasia by combining advanced magnetic resonance imaging data to intraoperative ultrasound, electrocorticography, and cortical stimulation: a preliminary experience. World Neurosurg 113:e738–e746 [PubMed: 29510282]

108. Humphreys RP, Hendrick EB, Hoffman HJ (1972) Cerebrovascular disease in children. Can Med Assoc J 107:774–776 [PubMed: 4565135]

109. VanamanMJ Hervey-Jumper SL, Maher CO (2010) Pediatric and inherited neurovascular diseases. Neurosurg Clin N Am 21:427–441 [PubMed: 20561493]

110. Ladner TR, Mahdi J, Attia A et al. (2015) A multispecialty pediatric neurovascular conference: a model for interdisciplinary management of complex disease. Pediatr Neurol 52:165–173 [PubMed: 25693581]

111. Banker BQ (1961) Cerebral vascular disease in infancy and child-hood. 1. Occlusive vascular diseases. J Neuropathol Exp Neurol 20:127–140 [PubMed: 13686597]

112. Scott RM, Smith ER (2009) Moyamoya disease and moyamoya syndrome. N Engl J Med 360:1226–1237 [PubMed: 19297575]

113. Acerbi F, Prada F, Vetrano IG et al. (2019) Indocyanine green and contrast-enhanced ultrasound videoangiography: a synergistic approach for real-time verification of distal revascularization and aneurysm occlusion in a complex distal middle cerebral artery aneurysm. World Neurosurg 125:277–284 [PubMed: 30776513]

114. Prada F, Del Bene M, Mauri G et al. (2018) Dynamic assessment of venous anatomy and function in neurosurgery with real-time intraoperative multimodal ultrasound: technical note. Neurosurg Focus 45:E6

115. Espagnet MCR, Bernardi B, Pasquini L et al. (2017) Erratum to: signal intensity at unenhanced T1-weighted magnetic resonance in the globus pallidus and dentate nucleus after serial administrations of a macrocyclic gadolinium-based contrast agent in children. Pediatr Radiol 47:1366 [PubMed: 28821897]

116. Du J, Li FH, Fang H et al. (2008) Microvascular architecture of breast lesions: evaluation with contrast-enhanced ultrasonographic micro flow imaging. J Ultrasound Med 27:833–842 [PubMed: 18499843]

117. Linden RA, Trabulsi EJ, Forsberg F et al. (2007) Contrast enhanced ultrasound flash replenishment method for directed prostate biopsies. J Urol 178:2354–2358 [PubMed: 17936814]

118. Sugimoto K, Moriyasu F, Kamiyama N et al. (2008) Analysis of morphological vascular changes of hepatocellular carcinoma by microflow imaging using contrast-enhanced sonography. Hepatol Res 38:790–799 [PubMed: 18507694]

119. Wilson SR, Jang HJ, Kim TK et al. (2008) Real-time temporal maximum-intensity-projection imaging of hepatic lesions with contrast-enhanced sonography. AJR Am J Roentgenol 190:691–695 [PubMed: 18287440]

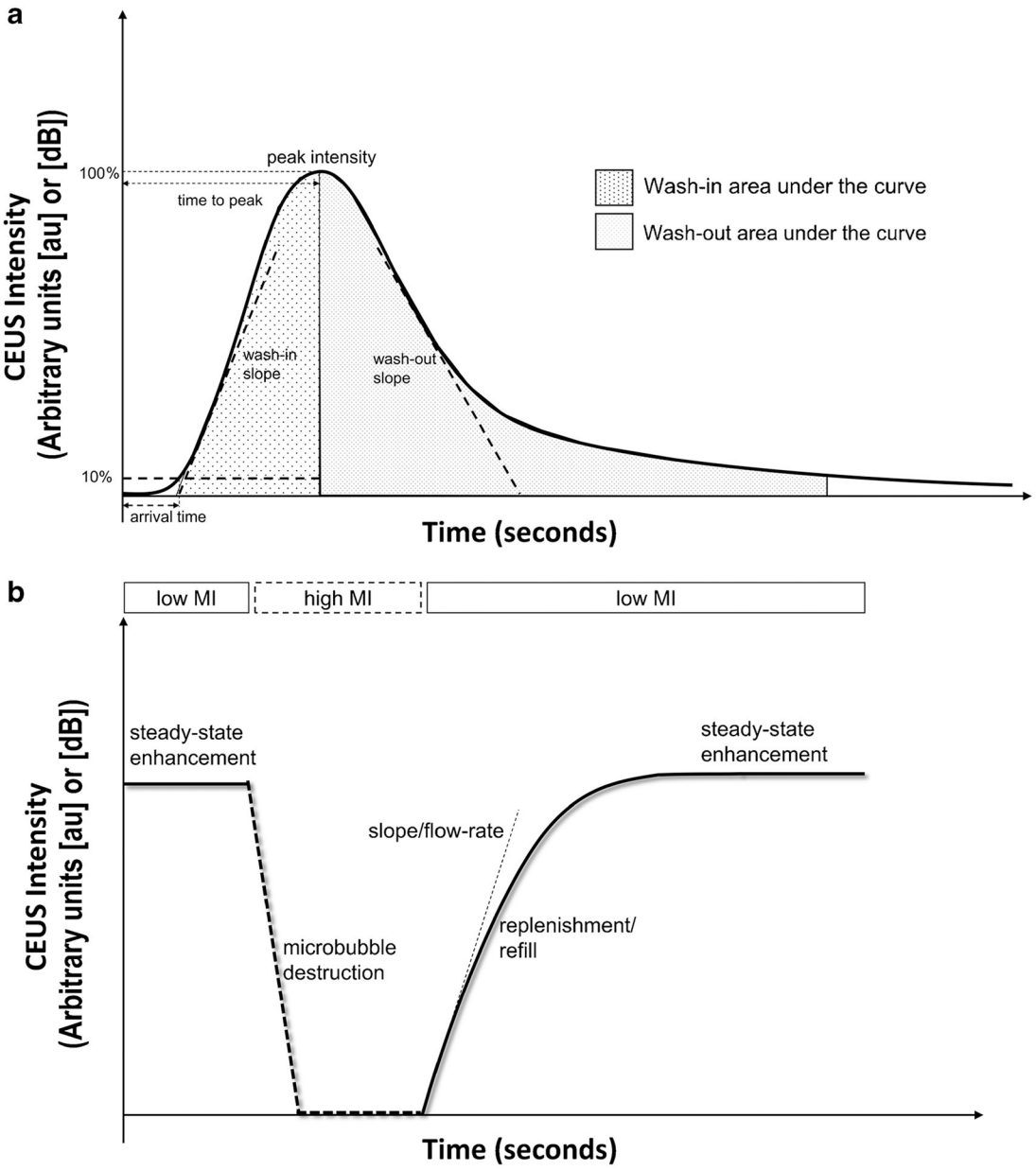

Fig. 1.

Contrast-enhanced ultrasound (CEUS) quantification methods: bolus-based time-intensity curve and infusion-based destruction-replenishment method. **a** Representative plot of a time-intensity curve generated from bolus administration of ultrasound contrast agent (UCA). The contrast agent intensity is represented by the solid line, with the intensity amplitude in arbitrary units (au) or decibels (dB) on the y-axis and time on the x-axis. Also shown are perfusion kinetics metrics of arrival time, time to peak, wash-in slope, wash-in area under the curve, washout area under the curve, washout slope and peak intensity that can be obtained from the time-intensity curve. **b** Representative plot of the UCA intensity changes over time using an infusion-based destruction–replenishment method. After infusion is initiated and using low mechanical index (MI) imaging, the UCA intensity gradually

increases until it reaches a steady-state enhancement (*solid line*). A high mechanical index pulse is then delivered, causing microbubble destruction within the imaging area of interest. The mechanical index is returned to a low setting to allow preservation of microbubbles washing into the field of view. The initial slope on the replenishment cycle can be used as an indicator of flow-rate or flux rate

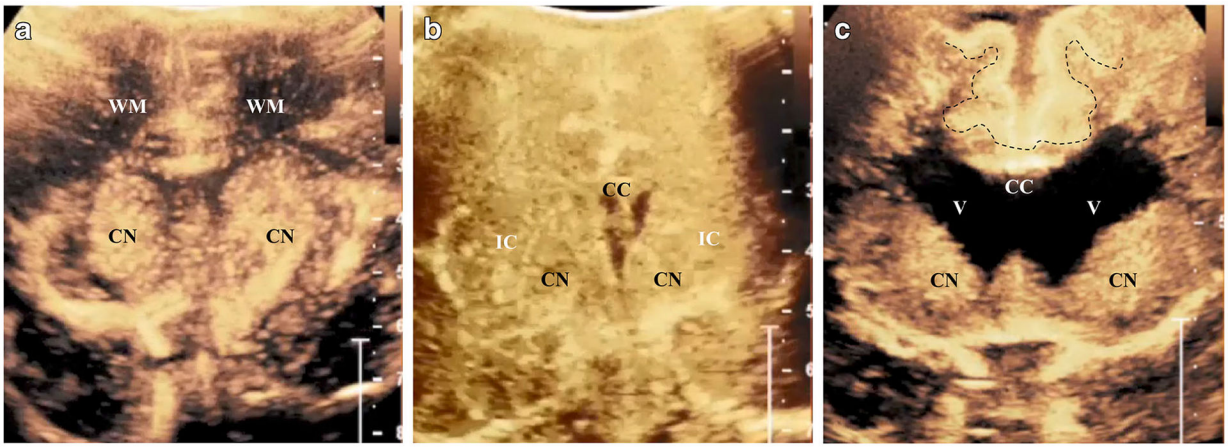

Fig. 2.

Contrast-enhanced ultrasound (CEUS) in normal brain and in hypoxic–ischemic injury. **a** Brain CEUS in a normal 1-month-old boy in the coronal plane demonstrates more avid perfusion to the central gray nuclei (*CN*) as compared to white matter (*WM*) during the wash-in phase. **b** Brain CEUS in a 14-day-old boy with known hypoxic–ischemic injury to the white matter. Image obtained in the coronal plane during the peak enhancement phase shows hyperenhancement of the internal capsule (*IC*) and corpus callosum (*CC*) during the reperfusion state. The degree of enhancement is like that of the central gray nuclei (*CN*), resulting in loss of differential perfusion between these structures. Central gray nuclei should be the most avidly enhancing structure at peak enhancement in infants. **c** Brain CEUS in a 10-month-old girl with known multiple hypoxic–ischemic insults to the brain. Image obtained in the coronal plane during wash-in phase shows mild ventriculomegaly (*V*) and avid perfusion of the cortical ribbon (*dashed line*), corpus callosum (*CC*) and central gray nuclei (*CN*). This finding predates the extensive laminar necrosis on follow-up MRI (not shown here)

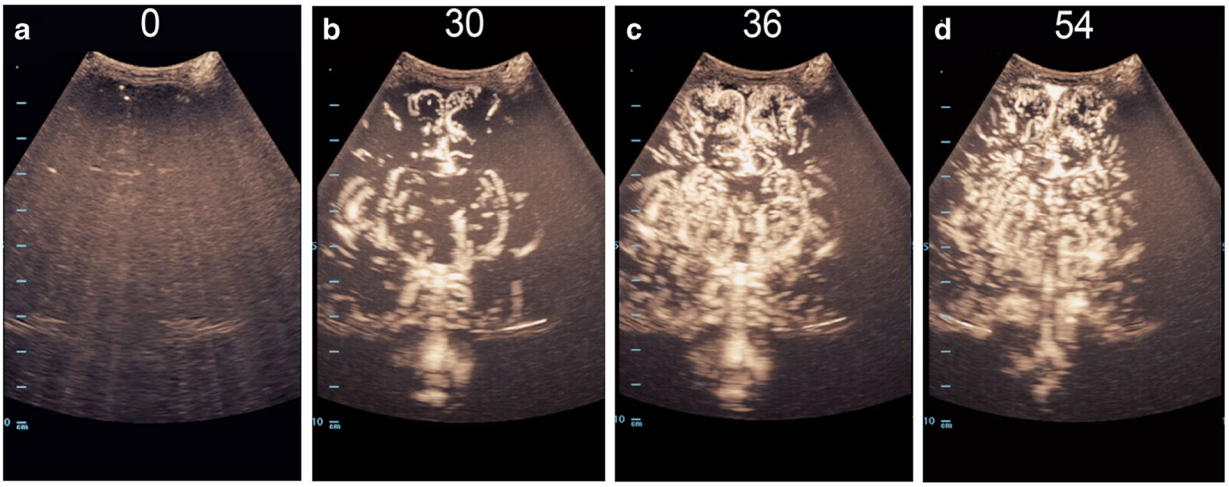

Fig. 3.

Maximum-intensity projection (MIP) images of cerebral vasculature. **a–d** Coronal MIP images of the cerebral vasculature in a 31-day-old girl with transposition ofthe great arteries during the arterial phase depict normal progressive arrival of the US contrast agent from 0 s (**a**) to 30 s (**b**), 36 s (**c**) and 54 s (**d**) post injection. Numbers on the upper aspect of each image represent the time, in seconds, following the administration of the US contrast agent

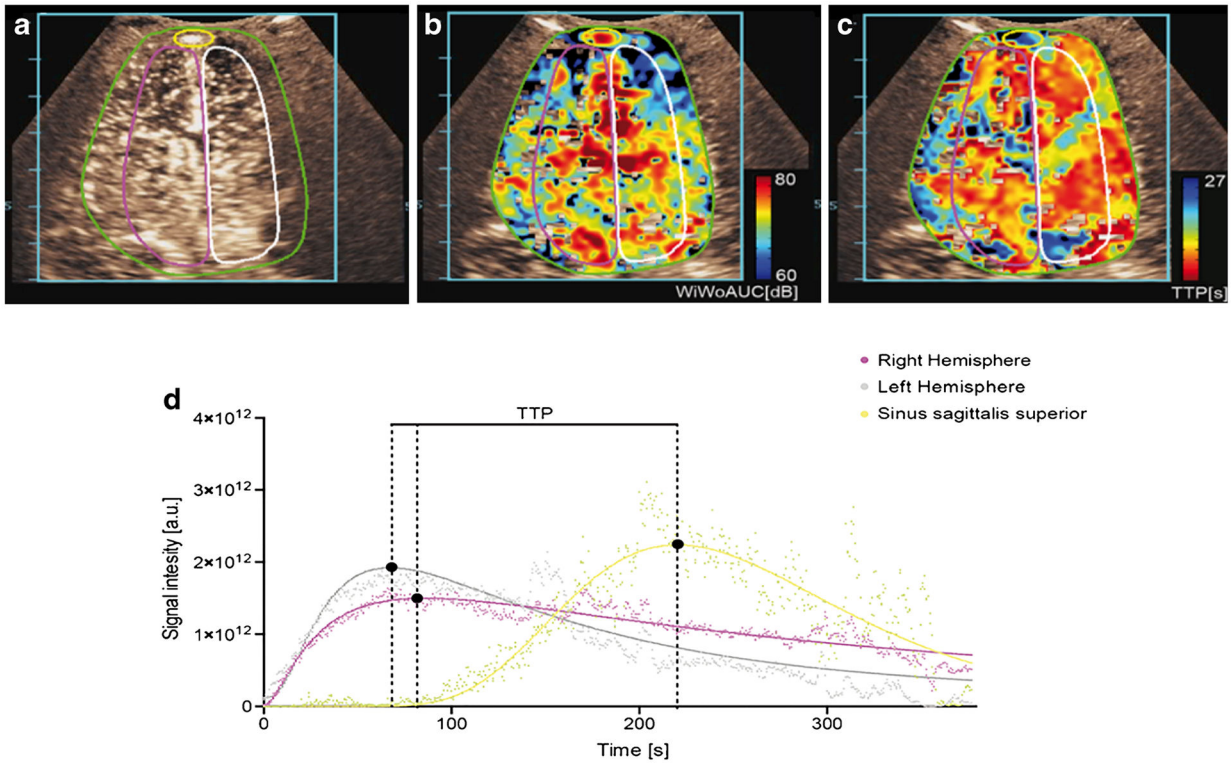

Fig. 4.

Visualization of dynamic intracerebral flow characteristics. **a** Exemplary transfontanelle coronal contrast-enhanced ultrasound (CEUS) images in a 31-day-old girl with transposition of the great arteries taken before surgical intervention. Regions of interest (ROI) were set for both hemispheres (*green*), the right hemisphere (*purple*), the left hemisphere (*white*), and the superior sagittal sinus (*yellow*). **b**, **c** The corresponding color-coded maps in the coronal plane show the washin–washout area-under-the-curve signal (**b**) and the time to peak (**c**). Mild asymmetry in cerebral perfusion is evident. **d** Time-intensity curve generated from the ROIs. X-axis shows time in seconds and y-axis shows signal intensity in arbitrary units (a.u.). Graphs are shown for the right hemisphere (*purple*), left hemisphere (*gray*) and the superior sagittal sinus (*yellow*). Both hemispheres show similar flow patterns with similar quantitative parameters (time to peak is shown). In contrast, venous flow in the superior sagittal sinus shows later enhancement (increased time to peak), as expected

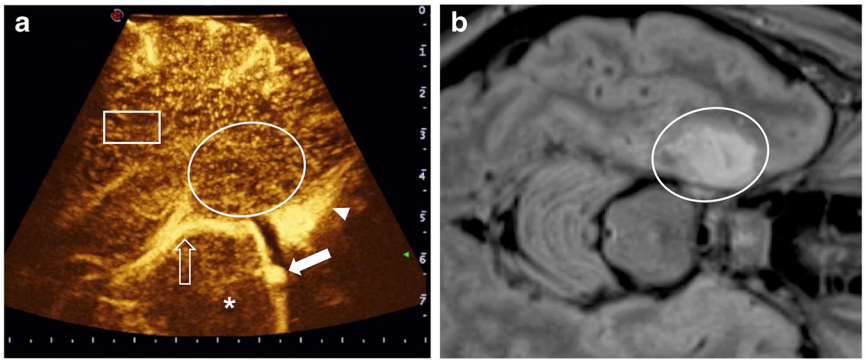

Fig. 5.

Fusion imaging for virtual navigation between the preoperative MRI and real-time contrast-enhanced ultrasound (CEUS), which was performed through a temporal craniotomy in a 15-year-old boy with dysembrioplastic neuroepithelial tumor (DNET). **a** Axial intraoperative CEUS image (near-field: right temporal lobe). **b** Co-planar axial fluid-attenuated inversion recovery MRI. The DNET in the medial right temporal lobe shows high intensity (*arrows* in **a**). The two imaging modalities are linked and the preoperative MRI follows the real-time CEUS as the US probe is tracked in the three-dimensional space. On CEUS the tumor shows a similar vascularization (*oval*) compared to the surrounding parenchyma (*rectangle*). Other anatomical structures visible on CEUS: the mesencephalon (*asterisk*), the cavernous sinus (*arrowhead*) and the basilar artery (*solid arrow*), and the posterior cerebral arteries (*open arrow*)

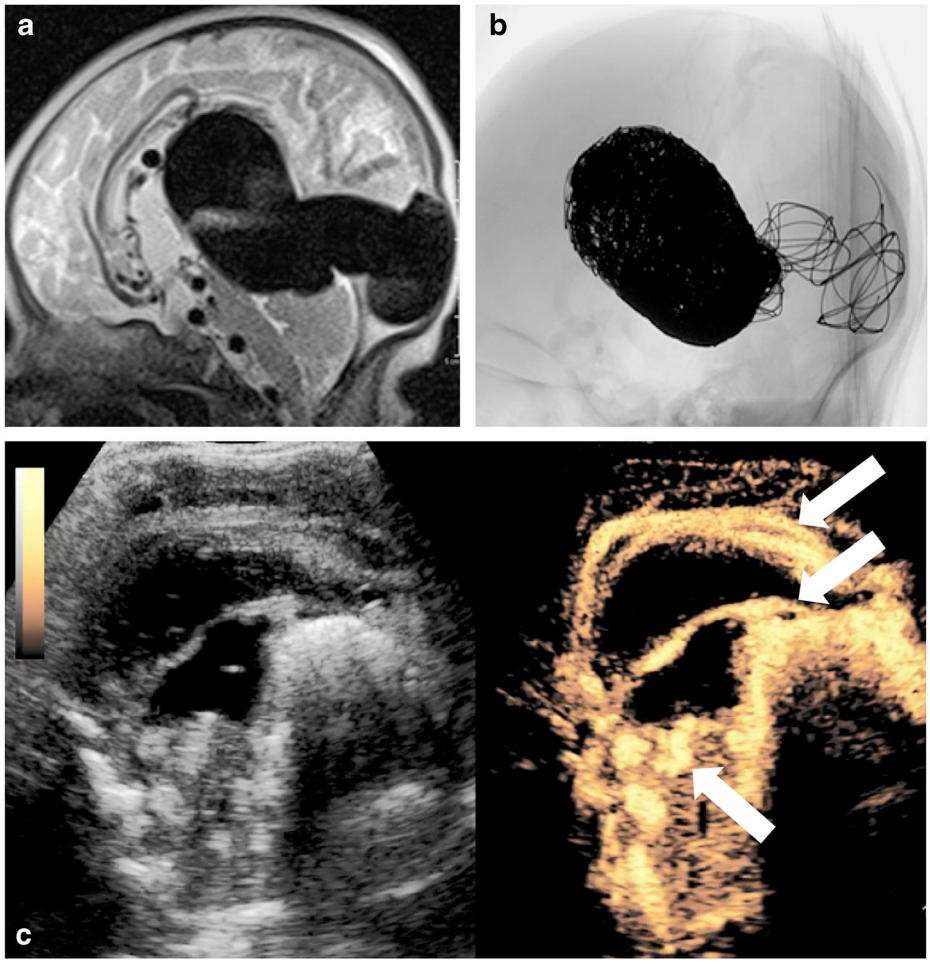

Fig. 6.

Contrast-enhanced ultrasound (CEUS) evaluation of a vein of Galen malformation post endovascular coiling in a 2-month-old boy. **a** Sagittal T2-weighted MRI brain sequence shows dark flow voids in the large arteriovenous malformation. **b** Fluoroscopic lateral image of the brain post endovascular coiling of the malformation. **c** Post-coiling sagittal CEUS with dual display of the gray-scale (*left*) and contrast-enhanced (*right*) modes obtained using the anterior fontanelle as the acoustic window to assess for residual flow in the coiled arteriovenous malformation. There is small-volume residual flow within the coiled malformation, with mildly prominent parasagittal vessels (*arrows*)